Source of Nonlinearity in Echo-Time-Dependent BOLD fMRI

Tao Jin,[1] Ping Wang,[1] Michelle Tasker,[1] Fuqiang Zhao,[2] and Seong-Gi Kim[1,2*]

Stimulation-induced changes in transverse relaxation rates can provide important insight into underlying physiological changes in blood oxygenation level-dependent (BOLD) contrast. It is often assumed that BOLD fractional signal change ($\Delta S/S$) is linearly dependent on echo time (TE). This relationship was evaluated at 9.4 T during visual stimulation in cats with gradient-echo (GE) and spin-echo (SE) echo-planar imaging (EPI). The TE dependence of GE $\Delta S/S$ is close to linear in both the parenchyma and large vessel area at the cortical surface for TEs of 6–20 ms. However, this dependence is nonlinear for SE studies in the TE range of 16–70 ms unless a diffusion-weighting of $b = 200$ s/mm^2 is applied. This behavior is not caused by inflow effects, T_2* decay during data acquisition in SE-EPI, or extravascular spin density changes. Our results are explained by a two-compartment model in which the extravascular contribution to $\Delta S/S$ vs. TE is linear, while the intravascular contribution can be nonlinear depending on the magnetic field strength and TE. At 9.4 T, the large-vessel IV signal can be minimized by using long TE and/or moderate diffusion weighting. Thus, stimulation-induced relaxation rate changes should be carefully determined, and their physiological meanings should be interpreted with caution. Magn Reson Med 55: 1281–1290, 2006. © 2006 Wiley-Liss, Inc.

Key words: fMRI; BOLD; TE dependence; spin-echo; gradient-echo; 9.4 T; linearity

In blood oxygenation level-dependent (BOLD) studies, stimulation-induced transverse relaxation rate changes (ΔR_2 in spin-echo (SE) and ΔR_2* in gradient-echo (GE) measurements) are directly related to susceptibility changes caused by variation in the paramagnetic deoxyhemoglobin content. Quantification of ΔR_2 or ΔR_2* can therefore provide useful insight into underlying physiological changes induced by neural activation. By combining this information with measurements of cerebral blood flow (CBF) and/or blood volume (CBV), one can determine oxygen consumption changes based on biophysical models (1–3). To determine stimulation-induced ΔR_2 or ΔR_2*, a linear relationship between fractional signal change ($\Delta S/S$) and echo time (TE) is commonly assumed. In SE studies this relationship can be expressed as

$$\Delta S/S = -TE \cdot \Delta R_2, \quad [1]$$

while in GE studies, $\Delta S/S = -\mathrm{TE} \cdot \Delta R_2$*. The underlying assumption for Eq. [1] is that the BOLD signal change is small and the signal decay can be described by a single (apparent) transverse relaxation rate, R_2. In a few experimental studies on the TE dependence of $\Delta S/S$ (4–10), a linear dependence on TE was found in brain parenchyma. However, several research groups found that linear extrapolation of $\Delta S/S$ to TE = 0 yielded a positive intercept in SE studies, which was usually ascribed to non-T_2 effects, such as inflow, T_2* contributions in SE echo-planar imaging (EPI), or elevation in the extravascular proton density during brain activation (4–8). Alternatively, a nonzero intercept may also result from linear fitting to a nonlinear relationship between TE and $\Delta S/S$. It should be noted that most of these studies measured only three or four TEs over a relatively small TE range, and thus may not have had enough coverage to detect nonlinear behavior.

Equation [1] may inadequately characterize the BOLD signal change in certain circumstances, since the signal originates from both intravascular (IV) and extravascular (EV) components. If the relaxation rate changes in IV and EV pools are significantly different, the *apparent* relaxation rate change obtained by the single-compartment model (Eq. [1]) can depend on both TE and the volume fraction of the IV compartment. Specifically, simulations based on blood oxygenation studies have predicted a nonlinear dependence of the IV BOLD signal on TE, which should be observable at high field (5,11,12).

To investigate the origin of the positive intercept and to experimentally confirm the expected nonlinear behavior, we performed GE and SE studies at 9.4 T with a wide range of TE values using the well-established cat visual stimulation model. According to the intravoxel incoherent motion (IVIM) model (13), moderate diffusion weighting from Stejskal-Tanner (S-T) gradients (14) can greatly suppress the IV signal in an imaging voxel when the vascular structure is random, or in large vessels where the blood flow is laminar but the effect on extravascular tissue water signal is much smaller (15,16). Therefore, we applied diffusion weighting to determine whether the positive intercept is due to intravascular effects. We also compared our experimental results with simulations based on a two-compartment model.

MATERIALS AND METHODS

Two-Compartment BOLD fMRI Model

The IV BOLD signal was recently simulated as a function of TE at field strengths of 1.5 T and 4.7 T by Silvennoinen et al. (11), and from 1.5 T to 9.4 T by Duong et al. (5). A comprehensive modeling of BOLD signals with their inherent complexities was beyond the scope of this work, but signals from both IV and EV compartments should be

[1]Magnetic Resonance Research Center, Department of Radiology, University of Pittsburgh, Pittsburgh, Pennsylvania, USA.

[2]Department of Neurobiology, University of Pittsburgh, Pittsburgh, Pennsylvania, USA.

Grant sponsor: NIH; Grant numbers: EB003324; EB003375; RR17239; NS44589; EB002013.

*Correspondence to: Seong-Gi Kim, University of Pittsburgh, 3025 E. Carson St., Pittsburgh, PA 15203. E-mail: kimsg@pitt.edu

Received 26 July 2005; revised 3 March 2006; accepted 6 March 2006.

DOI 10.1002/mrm.20918

Published online 12 May 2006 in Wiley InterScience (www.interscience.wiley.com).

Table 1
Parameter Values in Two-Compartment Model Simulations

Parameter	Description	Value
τ_{ex}	Water exchange time	1 ms[a]
λ	Water content ratio of tissue and blood	1.03[b]
D	Diffusion coefficient of tissue water	0.8×10^{-3} mm^2/s[c]
D^*	Pseudo-diffusion coefficient of blood	20×10^{-3} mm^2/s[d]
V	Baseline blood volume fraction	2–8% (default 4%)
ΔV	Functional blood volume fraction change	0–0.6% (default 0)
Y	Baseline blood oxygenation level	0.65[d]
ΔY	Functional blood oxygenation change	0.025–0.15 (default 0.05)
$R_{2,tissue}$	Baseline tissue relaxation rate	25 s^{-1}[e]
$\Delta R_{2,tissue}$	Functional tissue relaxation rate change	–0.06 to –0.24 s^{-1} (default –0.18 s^{-1})

[a]From Refs. 20 and 23.
[b]From Ref. 38.
[c]See text.
[d]See text.
[e]From Ref. 6.

included in descriptions of TE-dependent BOLD signal changes. At 9.4 T, the contribution from arterial blood can be ignored. Since arterial blood volume is very small (~1%), and T_2 of arterial blood (40 ms) is almost identical to that of tissue (6), arterial dilation has a minimal TE-independent contribution to the BOLD signal change. Therefore, the BOLD signal originates from venous blood (hereafter referred to simply as blood) and tissue compartments. The normalized MR signal at TE in the presence of a diffusion-weighting gradient (b) consists of IV and EV signals (S_{IV} and S_{EV}, respectively):

$$S=S_{IV}+S_{EV}=V\cdot\exp(-TE\cdot R_{2,blood}-b\cdot D^*) +\lambda\cdot(1-V)\cdot\exp(-TE\cdot R_{2,tissue}-b\cdot D) \quad [2]$$

where V is the volume fraction of blood in an imaging voxel; $R_{2,\ blood}$ and $R_{2,\ tissue}$ are the R_2 ($=1/T_2$) values of blood and tissue, respectively; D^* is the pseudo-diffusion coefficient of blood; D is the diffusion coefficient of tissue water, measured to be $\sim 0.8 \times 10^{-3}$ mm^2/s; and λ is the ratio between water contents of tissue and blood (38). T_1 effects are ignored in this model because the T_1 values of blood and tissue (1.9 and 2.2 s) are similar at 9.4 T (17).

During brain activation, the BOLD fractional signal change originating from the changes in both IV and EV compartments is

$$\Delta S/S = (\Delta S_{IV} + \Delta S_{EV})/S, \quad [3]$$

where

$$\Delta S_{IV}=[(V+\Delta V)\cdot\exp(-TE\cdot\Delta R_{2,blood})-V]\cdot\exp(-TE\cdot R_{2,blood}-b\cdot D^*)$$

and

$$\Delta S_{EV}=\lambda\cdot[(1-V-\Delta V)\cdot\exp(-TE\cdot\Delta R_{2,tissue})-(1-V)]\cdot\exp(-TE\cdot R_{2,tissue}-b\cdot D).$$

Here ΔV is the blood volume change during activation (assuming that within an imaging voxel the tissue volume decreases by the same amount as the blood volume increases); $\Delta R_{2,\ blood}$ and $\Delta R_{2,\ tissue}$ are the stimulation-induced changes in the transverse relaxation rates of blood and tissue, respectively. This model ignores any changes in ADC during activation.

Blood R_2, as a function of the oxygenation level (Y) and the magnetic field (B_0), can be estimated by models based on chemical exchange or diffusion effects (18–21). These models provide similar results (21,22), so blood R_2 was determined by the Luz-Meiboom exchange model (18) in this study:

$$R_{2,blood}=\frac{1}{T_{2,blood}}=24+1125(1-Y)^2\cdot\left(1-\frac{2\tau_{ex}}{\mathrm{TE}}\tanh\frac{TE}{2\tau_{ex}}\right)\Big/\left(1-\frac{2\tau_{ex}}{40}\tanh\frac{40}{2\tau_{ex}}\right), \quad [4]$$

where τ_{ex} is the correlation time for water exchange between erythrocyte and plasma, which ranges from 1 to 10 ms (20,23–25), and the coefficients in the equation above were determined from Lee et al.'s (6) experimental data obtained at 9.4 T.

Computer Simulation of TE-Dependent BOLD Signals

To illustrate the qualitative behavior of the TE-dependent BOLD signal changes at 9.4 T and compare it with experimental results, we performed computer simulations using Eqs. [2]–[4] with the parameter values listed in Table 1. In our anesthetized animal study with ~33% O_2 inhalation, Y is assumed to be 0.65 during baseline, which is slightly higher than the value of 0.55–0.6 observed during normal awake conditions (26). Four parameters (V, ΔV, ΔY and $\Delta R_{2,\ tissue}$) were varied independently to determine their individual effect on TE-dependent BOLD responses in the absence of S-T gradients. One of the four parameters was varied, while the others were fixed at default values of V = 4%, $\Delta V = 0$, $\Delta Y = 0.05$, and/or $\Delta R_{2,\ tissue} = -0.18$ s^{-1}.

To then determine the effect of S-T gradients, the value for b was varied with all other parameters fixed. According to the IVIM model, the attenuation of intravascular blood signal due to S-T gradients is complicated and depends on different vascular structures and flow characteristics within the vessels. In principle, due to the difference in the flow velocity, small S-T gradients can suppress the blood signal from large surface vessels, while much larger gradients are needed to suppress signal from small venules and capillaries. For example, Jochimsen et al. (27) showed a 60–70% loss of IV BOLD signal when a weak diffusion weighting of b = 50 s/mm^2 was applied, while b = 200–400 s/mm^2 was needed to further suppress the remaining IV signal from the microvasculature. This suggested that D^* could be more than 50×10^{-3} mm^2/s for large veins, but less than 10×10^{-3} mm^2/s for microvessels. For simplicity we assumed a simple monoexponential dependence of blood signal on b-value with a D^* value of 20×10^{-3} mm^2/s.

Animal Preparation and Visual Stimulation

A total of 15 female adolescent cats, weighing 0.7–2.0 kg, were studied under a survival experimental protocol approved by the Institutional Animal Care and Use Committee of the University of Pittsburgh. Nine and six animals were used for SE and GE studies, respectively. The animals were intubated and artificially ventilated under 0.8−1.3% isoflurane anesthesia in a 2:1 air:O_2 mixture. An intravenous catheter was inserted into the cephalic veins to continuously infuse ~0.2 mg/kg/hr pancuronium bromide. The animals were placed in a cradle and restrained in a normal postural position by an in-house-made head frame with bite and ear bars. The end-tidal CO_2 level was kept within normal physiological range (3.5% ± 0.5%) by adjusting the respiration rate and volume, and the rectal temperature was controlled at 38.5°C ± 0.5°C using a water-circulating pad. The animals were presented with high-contrast stationary vertical square-wave gratings with a spatial frequency of 0.15 cycle/degree during the baseline period. For the stimulation period the gratings moved at a temporal frequency of two cycles per second. Neural activation unrelated to the grating motion is minimal with this paradigm (28). The animals were inside the magnet for 4–5 hr per study. While most studies were performed on different animals, three animals were studied twice with at least a 7-day interval between consecutive studies.

MR Experiments

All NMR experiments were performed on a 9.4 T/31-cm horizontal magnet (Magnex, UK) interfaced to a Unity INOVA console (Varian, Palo Alto, CA, USA). The actively shielded 12-cm-diameter gradient insert (Magnex, UK) operates at a maximum gradient strength of 40 gauss/cm and a rise time of 130 μs. A 1.6-cm-diameter surface coil was placed on the top of the head. Fast low-angle shot (FLASH) images were obtained to identify the anatomical structures in the brain and to place the region of interest (ROI) in the isocenter of the magnetic field. Magnetic field homogeneity was optimized by localized shimming over a ~$10 \times 5 \times 5$ mm^3 volume to yield a water spectral linewidth of 15–25 Hz.

Multislice "scout" GE-EPI BOLD fMRI studies were performed, and a single 2-mm coronal plane perpendicular to the surface of the cortex, which gave a high-quality echo-planar image and a robust fMRI response, was chosen. All subsequent experiments were conducted on that slice with a 2×2 cm^2 field of view (FOV) and a 2-mm thickness. For anatomical reference, a T_1-weighted image was acquired by four-shot SE EPI with inversion recovery time = 1.4 s, repetition time (TR) = 5.4 s, TE = 18 ms, and matrix = 128×128.

Multiple-TE SE and GE fMRI experiments were then performed. All images were acquired by single-shot EPI with matrix size = 64×64, TR = 1.2 s for SE and 0.5 s for GE, and acquisition time = 32 ms. To obtain data from eight TE values with reasonable temporal resolution, two different four-TE series were interleaved. In each series/scan, images with four TE values were acquired sequentially, and the total scan time in a series was 4.8 s for SE and 2.0 s for GE fMRI. The TE order (in each series) was pseudo-randomized for each study. In SE fMRI experiments the stimulation paradigm (single block design) included 10 baseline (48 s), 10 stimulation, and 10 baseline images for each TE value, with 1–1.5 min of resting time between repetitive scans. In the GE fMRI experiments the stimulation paradigm included 20 baseline (40 s), 15 stimulation, and 20 baseline images for each TE value, with a 1-min rest between each scan.

Eight-TE SE fMRI Without and With S-T Gradients

Twelve studies were performed for eight-TE SE fMRI either without (N = 6) or with (N = 6) diffusion-weighting gradients. A double-echo EPI sequence was used with adiabatic half- and full-passage pulses (6); the 90° excitation pulse was not slice-selective, but the two 180° refocusing pulses were slice-selective. Two different four-TE series without S-T gradients consisted of interleaved TE values of 16, 20, 25, and 30 ms, and 55, 60, 65, and 70 ms. For diffusion-weighted experiments, two unipolar gradients along all three axes were placed on both sides of the second 180° pulse. The b-value of the S-T gradients was 200 s/mm^2 (corresponding to a first gradient moment M_1 of 1680 s/m), which is sufficient to suppress most of the IV signal (15,16,27). A TE value of 16 ms was not achievable with the inclusion of S-T gradients in our SE studies; two different TE series of 20, 25, 30, and 35 ms, and 55, 60, 65, and 70 ms were interleaved. For TE ≤ 35 ms, the zero k-space line was shifted 26–28 lines from the center of the data acquisition period to enable shorter TE values. Studies without and with diffusion weighting were performed separately due to time restrictions. Data sets were averaged in each study to improve the signal-to-noise ratio (SNR), with 15 data sets for b = 0 and ~20 data sets for b = 200 s/mm^2.

Eight-TE GE fMRI Without S-T Gradients

For GE experiments without diffusion-weighting gradients (N = 6 animals), the RF power of the slice-selective excitation pulse was optimized to maximize the steady-state

signal. Two different four-TE series were interleaved in each experiment: TE series of 6, 8, 10, and 12 ms, and 14, 16, 18, and 20 ms. To reduce the minimum TE, the zero *k*-space line was shifted by 26 lines from the center of the data acquisition period for TE $\leq$ 12 ms, and by 12 lines for TE $\geq$ 14 ms. Approximately 25 data sets were averaged for each study.

fMRI Data Analysis

Data analysis employed the STIMULATE software package (29) and programs written in Matlab®. With the sequential data sampling, images acquired at different TE values were obtained at different time points. To avoid erroneous results when we analyzed the dynamic signal change, we first grouped images with same TE together, and then applied linear temporal-interpolation to take into account their different time origins. Student's *t*-test maps were calculated for the averaged data set. A *t*-value threshold of 2 and minimal cluster size of four pixels were applied to the map.

For quantitative analyses, one ROI was assigned to be the entire active region from fMRI maps, which contains all activated pixels passing the *t*-value and cluster size thresholds. For that purpose, fMRI maps detected at TE = 30 ms and 12 ms were chosen for SE and GE studies, respectively. In addition, a middle cortical ROI and a cortical surface ROI were hand-traced with 1–2-pixel thickness to encompass approximately the middle one-third and the surface one-third of the cortex, respectively. Since the SE fMRI studies were performed separately without and with the S-T gradients, ROIs were also separately chosen for these data. Fractional signal changes were determined within the same ROIs for all TE values. To calculate the fractional signal change in SE (GE) experiments, the baseline periods were defined as the initial 43 s (38 s) of prestimulation data, while the activation periods were defined as data from 10 s to 48 s (6–30 s) after the onset of stimulation. The fractional signal change ($\Delta S/S$) was linearly fitted against TE to determine the intercept and slope.

To compare our experimental results with the two-compartment model simulation, we also calculated the contrast-to-noise ratio (CNR) for each TE value, which is the signal difference (ΔS) between the baseline and activated period divided by the standard deviation (SD) of the baseline state. To minimize cross-animal variance, TE-dependent CNR values from each animal were first normalized to the corresponding maximum value, and then averaged across animals. The SNR of the baseline images was also calculated. All data (including figures) are reported as the mean $\pm$ SD.

RESULTS

Simulation of the TE-Dependent BOLD Signal Using the Two-Compartment Model

The 9.4 T simulation results are presented in Fig. 1. In Fig. 1a–d, single parameters were varied as indicated, while other parameter values were fixed as listed in Table 1; there were no S-T gradients in these simulations. It should be noted that when τ_{ex} = 5 ms, the results were qualitatively very similar to τ_{ex} = 1 ms, and also when Y = 0.7, results were similar to Y = 0.65. In these figures, the overall dependence of $\Delta S/S$ on TE is nonlinear, and the deviation from linearity is more severe when the contribution of the IV compartment to the BOLD signal is relatively large compared to the EV signal, such as when $\Delta R_{2,tissue}$ is small, or when V, ΔV or ΔY is large. Linear dependence is achieved only when the intravascular contribution is negligible, such as when TE > 50 ms, or when it is significantly reduced by S-T gradients (Fig. 1e, b = 200 s/mm^2).

For comparison with the experimental CNR, absolute signal change (ΔS) was calculated for the four select cases shown in Fig. 1f. When the intravascular contribution is negligible (blue dashed curve, b = 200 s/mm^2), the optimum TE value for maximizing CNR is equal to the tissue T_2 value (40 ms). As the IV contribution becomes increasingly significant (b = 0 curves), the maximum contrast appears at a much shorter TE value.

SE fMRI With Eight TE Values

Figure 2a shows *t*-value maps of one animal from data obtained at TE = 30 ms without diffusion weighting. A large activated area of ~400 pixels can be seen in the gray matter area, which is depicted by the green contour in Fig. 2c. With a diffusion weighting of b = 200 s/mm^2 (Fig. 2b, same animal as in 2a), slightly fewer activated pixels and weaker activation were detected compared to images without diffusion weighting. In Fig. 2c, yellow pixels indicate the cortical surface ROI, while red pixels indicate the middle cortical ROI. On average, for b = 0 (N = 6) the cortical surface ROI consists of 141 $\pm$ 8 pixels and the middle cortical ROI consists of 156 $\pm$ 12 pixels. For b = 200 s/mm^2 (N = 6), the sizes are 133 $\pm$ 33 and 150 $\pm$ 13 pixels for surface and middle ROIs, respectively.

The TE dependence of BOLD fractional signal change for SE data from three ROIs is shown in Fig. 3a for b = 0 and 3b for b = 200 s/mm^2. For each ROI the slope (ΔR_2) and the intercept were calculated by linear fitting. For data with b = 0, there is an unambiguously nonlinear dependence of $\Delta S/S$ (and the slope and intercept) on the TE range: for TE $\leq$ 30 ms, the slope is much lower and the intercept is much higher than for TE $\geq$ 55 ms. A paired *t*-test (N = 6) shows significant differences between slopes of TE $\leq$ 30 ms vs. TE $\geq$ 55 ms, with P = 0.015 for the middle and $P < 0.001$ for the surface cortical ROI. In contrast, when b = 200 s/mm^2 the TE dependence becomes fairly linear for all three ROIs. The linear fitting results for data with TE $\geq$ 55 ms for b = 0 and 200 s/mm^2, and for all of the TE data with b = 200 s/mm^2 are shown in Table 2. ΔR_2 at the cortical surface (−0.146 s^{-1}) is ~27% smaller than at the middle of the cortex (−0.201 s^{-1}), in good agreement with previous results (30).

To minimize the cross-animal variation, $\Delta S/S$ at all TE values was normalized by the corresponding $\Delta S/S$ at TE = 70 ms, with results for the surface and middle cortical ROIs shown in Fig. 3c. There is an obvious difference between the linear dependence at b = 200 s/mm^2 and the nonlinear dependence at b = 0, which matches the two-compartment simulation data shown in Fig. 1e. Since baseline venous CBV (V) is higher for large vessels within

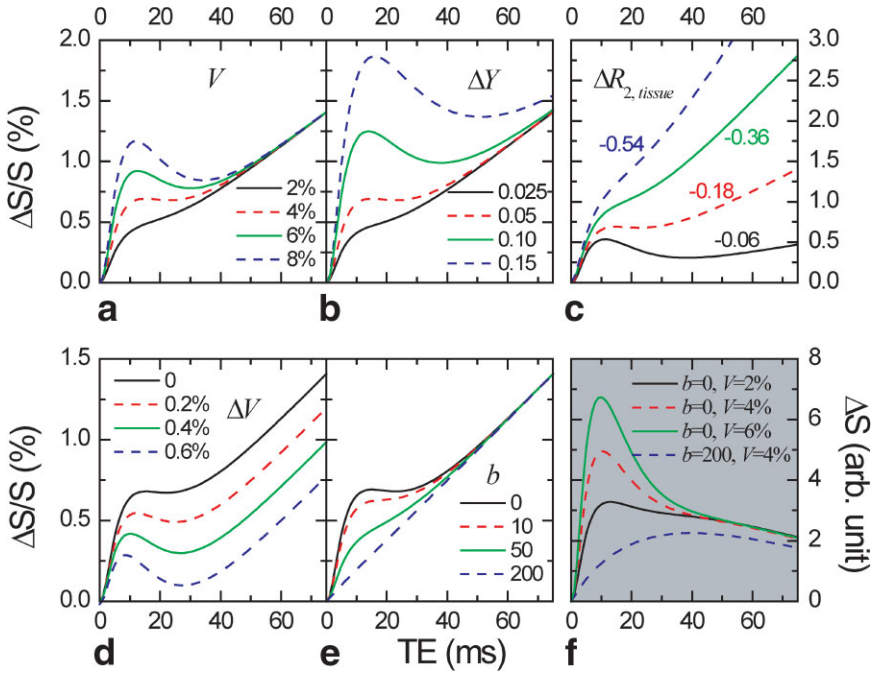

FIG. 1. Simulated results of $\Delta S/S$ vs. TE at 9.4 T based on the two-compartment model. Parameter values for (**a**) V, (**b**) ΔY, (**c**) $\Delta R_{2,\ tissue}$ (units of s^{-1}), (**d**) ΔV, and (**e**) b (units of s/mm^2) were varied, while other parameter values were fixed as listed in Table 1. **f:** ΔS vs. TE for four select cases; note the difference in vertical axis from other panels.

the cortical surface than at the middle of the cortex, when $b = 0$ the more prominent nonlinear behavior of the surface ROI is consistent with simulation data (Fig. 1a, 6% vs. 4%).

The IV contribution to the total BOLD signal change ($\Delta S_{IV}/S$) and the relative IV contribution ($\Delta S_{IV}/\Delta S$) can be quantitatively estimated from the difference between normalized $\Delta S/S$ data in Fig. 3c at $b = 0$ vs. 200 s/mm^2. The TE-dependence of $\Delta S_{IV}/\Delta S$ (obtained from $\Delta S_{IV}/S$ and $\Delta S/S$) is shown in Fig. 3d, with underlying assumptions that the signal change ($\Delta S/S$) detected at $b = 200$ s/mm^2 reflects $\Delta S_{EV}/S$, and that the IV contribution vanishes at TE = 70 ms for $b = 0$. When TE $\geq$ 55 ms, the IV signals are very small and thus the EV signals are dominant. With decreasing TE, $\Delta S_{EV}/S$ decreases linearly with TE, while $\Delta S_{IV}/\Delta S$ (and also $\Delta S_{IV}/S$) increases rapidly, reaching ~40% and 60% at TE = 20 ms for middle and surface cortical ROIs, respectively.

CNR and Activation Size

The dependence on TE can also be examined by determining the SNR and CNR. According to theory, the highest CNR should be observed by setting TE equal to the T_2 value of tissue. In the middle cortical ROI, the SNR of the baseline state images followed an exponential decay fairly well for both $b = 0$ and $b = 200$ s/mm^2 (data not shown). In contrast, the characteristics of the normalized CNR curves show a dependence on S-T gradients (Fig. 4a). For $b = 200$ s/mm^2 the peak appears to be located in the TE = 30–55 ms range, whereas for $b = 0$ the maximum CNR shifts to TE = 16–20 ms. The $b = 0$ experimental results resemble the behavior of the black curve in the two-compartment simulation of Fig. 1f, with a non-negligible IV contribution, while the $b = 200$ s/mm^2 data show a relative similarity to the blue dashed curve of Fig. 1f, in which the IV contribution is significantly suppressed. This finding is further supported by comparing the size of the activated area (also indicative of CNR) both without and with diffusion weighting, as illustrated in Fig. 4b.

GE fMRI With Eight TE Values

The TE dependence of the fractional signal change was also examined in BOLD GE with $b = 0$, and the results are shown in Fig. 5. For all three ROIs, most of the data points appear to be linearly dependent on TE, except at TE = 6 ms, where the slope appears to decrease. The results of a

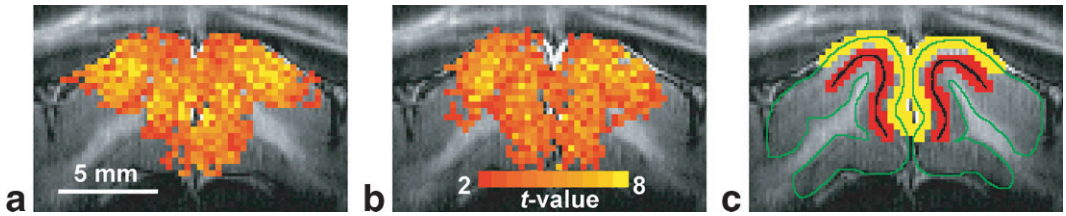

FIG. 2. Experimental BOLD SE t-maps for TE = 30 ms of a representative animal overlaid on T_1-weighted images, with $b = 0$ (**a**), and $b = 200$ s/mm^2 (**b**). **c:** The green contour indicates the gray matter area; hand-drawn cortical regions were traced (e.g., the black area for the middle of the cortex) and every pixel enclosed by or touching the traced lines were included for quantification; red and yellow pixels indicate the resulting ROIs at the middle and surface of the cortex, respectively.

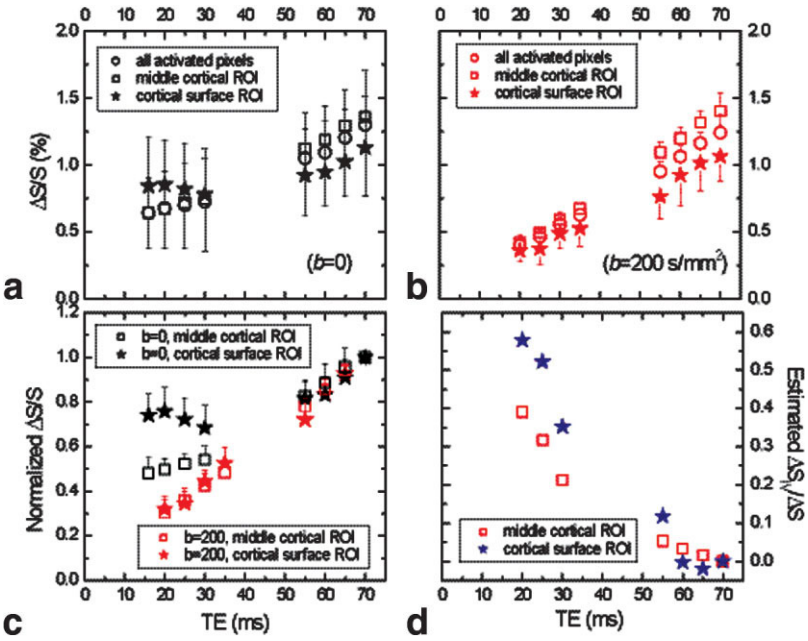

FIG. 3. $\Delta S/S$ vs. TE ($N = 6$) from three ROIs for SE data with $b = 0$ (**a**) and $b = 200$ s/mm^2 (**b**). The surface and middle cortical ROIs were chosen as depicted in Fig. 2c. **c:** $\Delta S/S$ was first normalized to values at TE = 70 ms for each data set, and then averaged across animals to minimize variation. **d:** $\Delta S_{IV}/\Delta S$ is estimated as a function of TE. The error bars, with only one side shown, indicate the SD.

linear fit to the data points with TE > 6 ms are listed in Table 2. Note there is a nonzero intercept for all ROIs when $\Delta S/S$ is extrapolated to TE = 0. As expected, the dominant activation in GE appears at the cortical surface area for all TEs studied (maps not shown). The relaxation rate change, ΔR_2^*, at the surface (-0.82 s^{-1}) is ~2.5 times that of the middle cortex (-0.34 s^{-1}). This agrees very well with previous results obtained by Zhao et al. (30) in experiments with similar parameters and TE = 10, 15, 20, and 25 ms.

DISCUSSION

Nonlinear TE-Dependent BOLD Responses

The nonlinear $\Delta S/S$ vs. TE dependence observed in our BOLD fMRI experiments can be explained by the simple two-compartment model. As shown by our results, the SE BOLD signal at 9.4 T can be separated into an EV component that is a linear function of TE, and an IV component that is not. When the IV contribution to BOLD signal changes is much smaller than the EV contribution, a linear TE-dependence of $\Delta S/S$ is expected. The relative IV contribution to SE BOLD signal change is quite significant at short TE values, while it diminishes for TEs that are long relative to blood T_2, ~6 ms at 9.4 T with $Y = 0.65$ (6). According to our estimation (Fig. 3d), the IV contribution to the SE BOLD signal change in parenchyma is about 10% at TE = 40 ms (= $T_{2,\ tissue}$), which is only slightly higher than the results of Lee et al. (6), who found that the IV BOLD signal was negligible for rat somatosensory stimulation. In the GE BOLD studies the TE dependence of the BOLD signal change is nearly linear for the TE values of 6–20 ms. This can be explained if the EV contribution is much larger than the IV effect (see blue dashed curve in Fig. 1c), since the EV relaxation rate change is much more prominent in GE than in SE, especially in regions with large vessels (see Table 2). Additionally, the blood T_2^* value may be so short that the IV contribution is small

Table 2
ΔR_2 and Intercepts From Linear Fitting to SE and GE Data*

	All activated pixels	Middle cortical ROI	Cortical surface ROI
SE (TE ≥ 55 ms, $b = 0$)			
ΔR_2	–0.171 ± 0.063	–0.163 ± 0.091	–0.140 ± 0.055
Intercept	0.09 ± 0.30	0.22 ± 0.41	0.13 ± 0.39
SE (TE ≥ 55 ms, $b = 200$)			
ΔR_2	–0.194 ± 0.043	–0.210 ± 0.045	–0.199 ± 0.039
Intercept	–0.11 ± 0.20	–0.058 ± 0.21	–0.27 ± 0.11
SE (all TE, $b = 200$)			
ΔR_2	–0.170 ± 0.028	–0.201 ± 0.029	–0.146 ± 0.030
Intercept	0.05 ± 0.09	–0.01 ± 0.10	–0.04 ± 0.06
GE (TE > 6 ms, $b = 0$)			
ΔR_2^*	–0.51 ± 0.09	–0.34 ± 0.09	–0.82 ± 0.10
Intercept	0.56 ± 0.39	0.53 ± 0.37	0.83 ± 0.63

*The unit of the intercept is % and of ΔR_2 and ΔR_2^* is s^{-1}. Note the $b = 0$ and 200 s/mm^2 SE data were obtained separately.

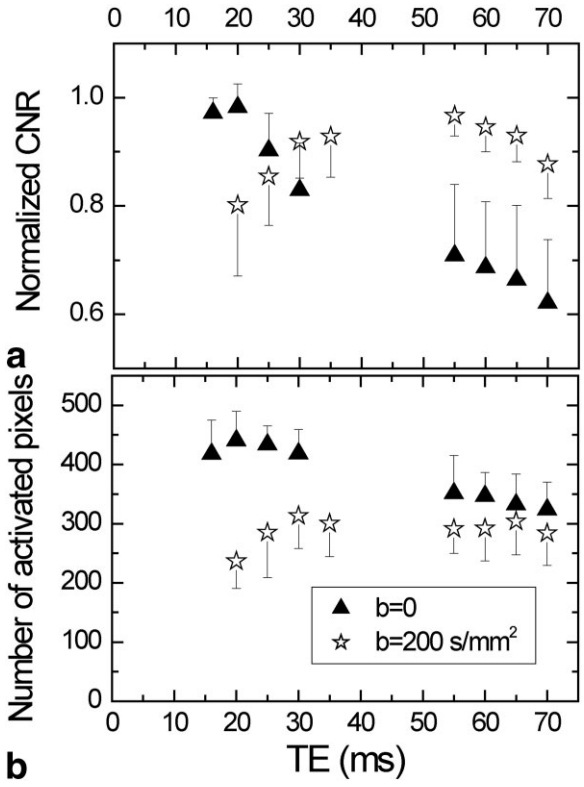

FIG. 4. **a:** Normalized CNR as a function of TE for BOLD SE data ($N = 6$) with $b = 0$ and $b = 200$ s/mm^2; data were obtained from the middle cortical ROI. Here CNR is the ratio between the signal change (ΔS) and SD of the baseline signal. **b:** TE dependence of the averaged number of activated pixels ($N = 6$) from the t-map for $b = 0$ and $b = 200$ s/mm^2.

even at TE ~ 6 ms. To detect the subtle nonlinear behavior shown in the blue dashed line in Fig. 1c, a wider TE range may be needed. Positive intercepts in our GE BOLD signals are possibly due to IV contribution and/or inflow effect. Further studies (such as experiments with vs. without S-T gradients) are needed to determine the exact source of the positive intercepts in GE BOLD signals.

Even if the IV contribution is dominant, linear TE dependence can be observed if the IV BOLD signal is linear within the range of TE values used for fMRI studies (see simulation data with TE < 10 ms in Fig. 1a–d). Assuming $\Delta V = 0$ and a small relaxation rate change (ΔR_2) during activation for both blood and tissue water, the BOLD fractional signal changes for both compartments in Eq. [3] when $b = 0$ can be expressed as

$$\Delta S_{IV}/S \approx -V \cdot TE \cdot \Delta R_{2,blood} \cdot \exp[TE \cdot (R_{2,tissue} - R_{2,blood})];$$

and

$$\Delta S_{EV}/S \approx -\lambda \cdot TE \cdot \Delta R_{2,tissue}.$$

For the IV compartment, the linearity of the TE dependence is determined by the exponential term, which in turn depends on the relaxation rate difference between tissue and blood water during the baseline state (linearity only occurs when $TE \cdot |R_{2,\,tissue} - R_{2,\,blood}| << 1$). At 9.4 T the relaxation rate difference is –142 s^{-1}, assuming tissue and blood T_2 values of 40 and 6 ms (6), which leads to a nonlinear TE dependence. However, assuming that T_2 values of tissue and blood at 1.5 T are 90 ms (31) and 130 ms (25), respectively, the relaxation rate difference is 3.4 s^{-1}, leading to a nearly linear dependence between TE = 0 and 100 ms. Our simulations at 1.5 T in the TE range of 0–150 ms (results not shown) confirmed a nearly linear dependence for 1.5 T, while the linearity for 3 T is highly dependent on the parameter τ_{ex} (the TE-dependence is nearly linear for $\tau_{ex} = 1$ ms but is nonlinear for $\tau_{ex} = 5$ ms). Hulvershorn et al. (32) performed similar simulations for both IV and EV compartments at 3 T, and compared τ_{ex} values from 0.5 to 10 ms. Their experimental results were nearly linear between TE = 30 and 70 ms with a small intercept of ~0.2%, and agreed better with simulations at $\tau_{ex} = 0.5$ ms.

When S-T gradients were applied ($b = 200$ s/mm^2) in our study, a nearly linear TE-dependence was observed, supporting the conclusion that the source of nonlinearity is a change of the IV signal during stimulation. If the CBV change is significant and the IV contribution is completely removed, a negative intercept is expected (see simulation data with TE > 40 ms in Fig. 1d). In our experimental data with $b = 200$ s/mm^2, the intercepts are negative for TE ≥ 55 ms data, but are almost zero with the inclusion of shorter-TE data (Table 2). The negative intercept for TE ≥ 55 ms may reflect the CBV change, while the near-zero intercept for all of the TEs indicates an incomplete suppression of the IV contribution. It is known that a b-value of 200 s/mm^2 does not completely suppress all IV BOLD signals, especially in the small capillaries where blood flow is slow. Complete removal of IV signals may be achievable at lower fields by the recently developed blood-nulling method based on the T_1 difference between tissue and blood water (33). Note that at 9.4 T the T_1's of tissue and blood water (1.9 s vs. 2.2 s) converge (17), which makes blood-nulling more difficult.

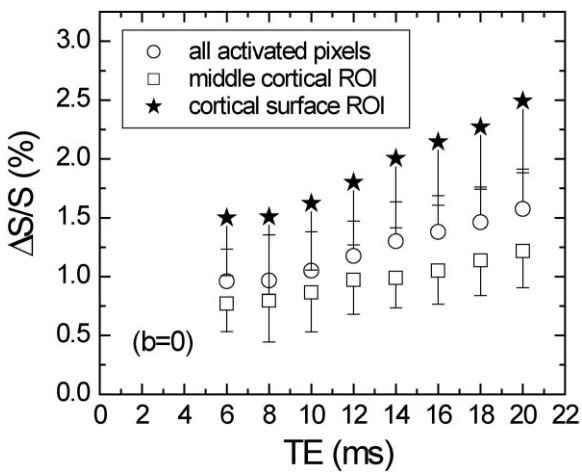

FIG. 5. $\Delta S/S$ vs. TE from three ROIs for BOLD GE data ($N = 6$) without S-T gradients. The ROIs (not shown) were chosen in a manner similar to that used for the SE data.

Linear TE-Dependent BOLD Responses

If contributions from either inflow, T_2* decay during SE-EPI acquisition, or EV spin density changes are significant, then linear TE dependence with a nonzero intercept is expected (4–8). However, these effects cannot explain the nonlinear TE dependence of BOLD signal changes observed in our SE experiments. A nonzero intercept of $\Delta S/S$ when extrapolated to TE = 0 can also result from a linear fit to nonlinear data. From our SE results without S-T gradients in the middle of the cortex, the intercept was 0.22% after a linear fit to data for TE ≥ 55 ms, but a forced linear fit to data in the TE = 16–30 ms range yields an increased intercept of 0.53% (Fig. 3a).

With the short TRs adopted in our EPI measurements (TR = 1.2 s for SE, and 0.5 s for GE), the water proton spins in the imaging slice did not achieve full T_1 (longitudinal) relaxation. As CBF increases during visual stimulation, more fresh (unexcited) proton spins enter the imaging slice and perturb the "steady state," giving rise to an increase in the signal change. The magnitude of this inflow effect decreases with increasing TR, and is independent of TE. Yacoub et al. (4) observed an intercept of 0.3–0.4% using SE BOLD at 7 T and an intercept of similar magnitude at 4 T. These intercepts were attributed to inflow effects because they could almost be eliminated using flow-suppression S-T gradients or an adiabatic 90° postacquisition pulse. This inflow effect probably contributes significantly to the large positive intercept in our GE results, with values of 0.83% and 0.53% in both the surface and middle cortical areas, respectively. However, for SE the 90° adiabatic excitation pulse we used was not slice-selective, and therefore during activation any change from steady-state magnetization should be minimal. As a result, the inflow effect is not expected to contribute significantly to the fractional signal change or the positive intercept. This was also confirmed by our experiments ($N = 3$, data not shown) in which $\Delta S/S$ was found to be almost identical for TR values of either 1 s or 2 s.

Our EPI acquisition time is relatively long (32 ms), and is comparable to tissue T_2* (~30 ms). T_2* decay during data acquisition is more significant for the high k-space lines at the edge of the readout window. Hence, there is an intrinsic T_2* blurring effect in SE-EPI. This is also referred as a T_2' effect since $R_2^* = R_2' + R_2$ (where $R_2' = 1/T_2'$). For SE-EPI fMRI studies, the observed signal change would be affected in a similar way if there is a T_2' change during activation. If the same EPI readout window is used for multiple TEs, the blurring effect (i.e., the point spread function (PSF)) will be the same. Thus, the T_2* effect should be TE-independent, as indicated by Golay et al.'s (34) T_2 measurements. For SE-EPI fMRI studies with multiple TE values, ΔR_2 is normally obtained from the slope of a linear fit, while the intercept at TE = 0 is presumed to yield $\Delta R_2'$ if other contributions, such as blood volume changes, IV signal changes, and inflow effects, are negligible. Some preliminary simulation and experimental results suggest that a significant portion of the SE signal change during activation could be due to changes in T_2', depending on field strength, activation size, and spatial resolution (35–37). Therefore, it is necessary to estimate how large the effect of a T_2' change would be on our SE results. One might be prompted to speculate that significant signal changes at the cortical surface are mostly due to T_2' changes. Moreover, if one looks only at the short-TE data (16 ≤ TE ≤ 30 ms) in Fig. 3a, it might appear that the signal change at the cortical surface is caused solely by T_2' changes (the large intercept), while the almost flat slope indicates a negligible T_2 change. However, this is inconsistent with the data at TE ≥ 55 ms, which show significantly steeper slopes and much smaller intercepts. When intravascular contributions are minimized with b = 200 s/mm^2 (Fig. 3b and Table 2), the slope across the entire TE span becomes similar, and the intercept is very small for both parenchymal and surface ROIs. Therefore, in our studies the significant nonzero intercept at short TEs is primarily due to IV contributions rather than T_2' changes.

In human studies at 1.5 and 3 T, Stroman et al. (7,8) found the intercept to be 0.66–1.0% with SE-EPI and 0.11–0.35% with GE-EPI, and this intercept was hypothetically attributed to an increase in the EV water proton density. Their hypothesis disagreed with the 3 T results of Jochimsen et al. (9), who found that the intercept was near zero for SE and about −0.1% for a stimulated-echo sequence. If an EV proton density increase during activation was a major contributor to the large positive intercept in our short TE data (16 ≤ TE ≤ 30 ms), this effect should remain when S-T gradients are applied, and one would expect a similar intercept with b = 0 vs. b = 200 s/mm^2. However, our data do not show similar intercepts for these conditions, and thus do not support the notion that nonzero intercepts are caused by EV proton density increases.

Implications of Stimulation-Induced ΔR_2 Measurements

The accurate determination of stimulation-induced transverse relaxation rate changes is important for understanding the BOLD mechanism and underlying physiological changes. Most biophysical models use only relaxation changes in either the IV or the EV pool; however, to convert relaxation changes into physiological changes, it is essential to separate IV and EV signals. Since both IV and EV signals contribute to the measured BOLD change, their relative contribution depends on magnetic field strength and TE values. The ΔR_2 values calculated from TE ≥ 55 ms with b = 0 and from all TE values with b = 200 s/mm^2 are similar (Table 2). This suggests that two simple approaches can be used to separate the IV and EV BOLD signals: 1) the use of very long TE values, or 2) the application of moderate diffusion-weighting gradients. At very high fields, long-TE data are assumed to contain only EV pool contributions ($\Delta R_{2,\ tissue}$), and therefore can be linearly extrapolated to TE = 0. The difference in ΔR_2 between experimental data and extrapolated data at short TE values can then be attributed to the IV contribution ($\Delta R_{2,\ blood}$). Alternatively, the difference between data with and without diffusion-weighting gradients would represent the IV signal contribution, while the signal changes with diffusion-weighting gradients would originate from the EV pool. Note that these two approaches would work more accurately for large vessels at the cortical surface than for

capillaries. First, the diffusion weighting is less effective for suppressing the blood signal of small vessels, as discussed earlier. Second, the T_2 of capillary blood, with a higher oxygenation level, is longer than that of venous blood, and thus the blood signal of capillaries may remain at a longer TE.

CONCLUSIONS

We studied the TE dependence of SE and GE BOLD fractional signal changes at 9.4 T. Nonlinear TE dependence was observed for SE, with ΔR_2 and intercept values depending on the range of TE values. This is mostly due to IV contribution increases with TE decreases, and this finding agrees well with a two-compartment model simulation. At surface large vessel area, the IV signal can be effectively suppressed with a relatively long TE ($\geq$55 ms) and/or with moderate diffusion weighting of $b = 200$ s/mm^2. Longer TE and/or larger diffusion weighting may be needed to suppress the IV signal from capillaries. For GE, a nearly linear TE dependence with a large positive intercept is observed. This linear dependence is likely due to the EV contribution being dominant in the GE sequence. Our results provide experimental proof that application of the linear BOLD model is inaccurate, especially in high-field SE studies, due to nonlinear IV contributions. Therefore, the IV effect should be considered when ΔR_2 is calculated in BOLD experiments. Furthermore, EV and IV signals should be separated when fMRI biophysical mechanisms are examined.

ACKNOWLEDGMENT

The authors thank Kristy Hendrich for comments on the manuscript and for 9.4 T system support.

REFERENCES

1. Kim S-G, Ugurbil K. Comparison of blood oxygenation and cerebral blood flow effects in fMRI: estimation of relative oxygen consumption change. Magn Reson Med 1997;38:59–65.
2. Kim S-G, Rostrup E, Larsson HBW, Ogawa S, Paulson OB. Simultaneous measurements of CBF and CMRO2 changes by fMRI: significant increase of oxygen consumption rate during visual stimulation. Magn Reson Med 1999;41:1152–1161.
3. Lu H, Golay X, Pekar J, van Zijl PC. Sustained poststimulus elevation in cerebral oxygen utilization after vascular recovery. J Cereb Blood Flow Metab 2004;24:764–770.
4. Yacoub E, Duong TQ, Van De Moortele P, Lindquist M, Adriany G, Kim S-G, Ugurbil K, Hu X. Spin-echo fMRI in humans using high spatial resolutions and high magnetic fields. Magn Reson Med 2003;49:655–664.
5. Duong TQ, Yacoub E, Adriany G, Hu X, Ugurbil K, Kim S-G. Microvascular BOLD contribution at 4 and 7T in the human brain: gradient-echo and spin-echo fMRI with suppression of blood effects. Magn Reson Med 2003;49:1019–1027.
6. Lee S-P, Silva AC, Ugurbil K, Kim S-G. Diffusion-weighted spin-echo fMRI at 9.4 T: microvascular/tissue contribution to BOLD signal change. Magn Reson Med 1999;42:919–928.
7. Stroman PW, Tomanek B, Krause V, Frankenstein UN, Malisza KL. Functional magnetic resonance imaging of the human brain based on signal enhancement by extravascular protons (SEEP fMRI). Magn Reson Med 2003;49:433–439.
8. Stroman PW, Krause V, Frankenstein UN, Malisza KL, Tomanek B. Characterization of contrast changes in functional MRI of the human. Magn Reson Imaging 2001;19:827.
9. Jochimsen TH, Norris DG, Moller HE. Is there a change in water proton density associated with functional magnetic resonance imaging? Magn Reson Med 2005;53:470.
10. Menon RS, Ogawa S, Tank DW, Ugurbil K. 4 Tesla gradient recalled echo characteristics of photic stimulation-induced signal changes in the human primary visual cortex. Magn Reson Med 1993;30:380–386.
11. Silvennoinen M, Clingman CS, Golay X, Kauppinen RA, van Zijl PC. Comparison of the dependence of blood R2 and R2* on oxygen saturation at 1.5 and 4.7 Tesla. Magn Reson Med 2003;49:47–60.
12. Spees W, Yablonskiy D, Oswood M, Ackerman JH. Water proton MR properties of human blood at 1.5 Tesla: magnetic susceptibility, T1, T2, T*2, and non-Lorentzian signal behavior. Magn Reson Med 2001;45:533–542.
13. LeBihan D, Breton E, Lallemand D, Grenier P, Cabanis E, Laval-Jeantet M. MR imaging of intravoxel incoherent motions: application to diffusion and perfusion in nerologic disorders. Radiology 1986;161:401–407.
14. Stejskal EO, Tanner JE. Spin diffusion measurements: spin echoes in the presence of a time-dependent field gradient. J Chem Physics 1965;42:288–292.
15. Boxerman JL, Bandettini PA, Kwong KK, Baker JR, Davis TL, Rosen BR, Weisskoff RM. The intravascular contribution to fMRI signal change: Monte Carlo modeling and diffusion-weighted studies in vivo. Magn Reson Med 1995;34:4–10.
16. Song AW, Wong EC, Tan SG, Hyde JS. Diffusion-weighted fMRI at 1.5T. Magn Reson Med 1996;35:155–158.
17. Tsekos NV, Zhang F, Merkle H, Nagayama M, Iadecola C, Kim S-G. Quantitative measurements of cerebral blood flow in rats using the FAIR technique: correlation with previous iodoantipyrine autoradiographic studies. Magn Reson Med 1998;39:564–573.
18. Luz Z, Meiboom S. Nuclear magnetic resonance study of the protolysis of trimethyammonium ion in aqueous solution—order of the reaction with respect to solvent. J Chem Phys 1963;39:366–370.
19. Carr HY, Purcell EM. Effects of diffusion on free precession in nuclear magnetic resonance experiments. Phys Rev 1954;94:630–638.
20. Thulborn KR, Waterton JC, Mattews PM, Radda GK. Oxygenation dependence of the transverse relaxation time of water protons in whole blood at high field. Biochem Biophys Acta 1982;714:265–270.
21. Jensen JH, Chandra R. NMR relaxation in tissues with weak magnetic inhomogeneities. Magn Reson Med 2000;44:144–156.
22. Silvennoinen J. A study of NMR relaxation in blood—mechanistic considerations and implications for quantitative functional MRI. Kuopio: University of Kuopio; 2002.
23. Meyer M, Yu O, Eclancher B, Grucker D, Chambron J. NMR relaxation rates and blood oxygenation level. Magn Reson Med 1995;34:234–241.
24. Bryant R, Marill K, Blackmore C, Francis C. Magnetic relaxation of blood and blood clots. Magn Reson Med 1990;13:133–144.
25. Wright GA, Hu BS, Macovski A. Estimating oxygen saturation of blood in vivo with MR imaging at 1.5 T. J Magn Reson Imaging 1991;1:275–283.
26. Haacke EM, Lai S, Reichenbach JR, Kuppusamy K, Hoogenraad F, Takeichi H, Lin W. In vivo measurement of blood oxygen saturation using magnetic resonance imaging: a direct validation of the blood oxygen level-dependent concept in functional brain imaging. Hum Brain Mapp 1997;5:341–346.
27. Jochimsen TH, Norris DG, Mildner T, Moller HE. Quantifying the intra- and extravascular contributions to spin-echo fMRI at 3 T. Magn Reson Med 2004;52:724.
28. Harel N, Lee S-P, Nagaoka T, Kim D-S, Kim S-G. Origin of negative blood oxygenation level-dependent fMRI signals. J Cereb Blood Flow Metab 2002;22:908–917.
29. Strupp JP. Stimulate: A GUI based fMRI analysis software package. Neuroimage 1996;3:S607.
30. Zhao F, Wang P, Kim S-G. Cortical depth-dependent gradient-echo and spin-echo BOLD fMRI at 9.4T. Magn Reson Med 2004;51:518–524.
31. Breger RK, Rimm AA, Fischer ME, Papke RA, Haughten VM. T_1 and T_2 measurements on a 1.5 Tesla commercial imager. Radiology 1989;171:273–276.
32. Hulvershorn J, Bloy L, Gualtiere EE, Leigh JS, Elliott MA. A two compartment model for spin echo BOLD contrast: validation at 3T. In: Proceedings of the 12th Annual Meeting of ISMRM, Kyoto, Japan, 2004. p 1065.

33. Lu H, Golay X, Pekar J, Van Zijl P. Functional magnetic resonance imaging based on changes in vascular space occupancy. Magn Reson Med 2003;50:263–274.
34. Golay X, Silvennoinen M, Zhou J, Clingman CS, Kauppinen RA, Pekar J, van Zijl PC. Measurement of tissue oxygen extraction ratios from venous blood T2: increased precision and validation of principle. Magn Reson Med 2001;46:282–291.
35. Birn R, Bodurka J, Petridou N, Bandettini P. Experimental determination of the effect of T2′ changes in spin-echo EPI. In: Proceedings of the 12th Annual Meeting of ISMRM, Kyoto, Japan, 2004. p 997.
36. Birn R, Bandettini P. The effect of T2′ changes on spin-echo EPI-derived brain activation maps. In: Proceedings of the 10th Annual Meeting of ISMRM, Honolulu, HI, USA, 2002. p 1324.
37. Keilholz SD, Silva AC, Duyn J, Koretsky AP. The contribution of T2* to spin-echo EPI: implications for high-field fMRI studies. In: Proceedings of the 13th Annual Meeting of ISMRM, Miami, FL, USA, 2005. p 32.
38. Herscovitch P, Raichle ME. What is the correct value for the brain-blood partition coefficient for water? J Cereb Blood Flow Metab 1985; 5:65–69.